Simulating Multi-channel Vacuum Phototriodes using COMSOL

Sema Zahid[a,*], P.R Hobson[a] and D.J.A. Cockerill[b]

[a]*Brunel University London, Particle Physics Group, Department of Electronic and Computer Engineering, Uxbridge, UB8 3PH, UK*

[b]*Particle Physics Department STFC, Rutherford Appleton Laboratory, Harwell Campus, Didcot OX11 0QX, UK*

[1] *Corresponding author: Sema.Zahid@brunel.ac.uk*

Abstract

Vacuum phototriodes have been used for a number of years in particle physics experiments. For example, they were used in the OPAL experiment at LEP and are currently used in the endcap calorimeter of the CMS experiment at CERN's Large Hadron Collider. A simulation of a CMS vacuum phototriode (RIE type FEU-188) has been implemented using the COMSOL multi-physics software environment. In addition, a new vacuum phototriode configured with a segmented anode, to provide four independent channels within the same overall device envelope, is presented. The induced signal as a function of time, and the effects of cross-talk in adjacent quadrants have been studied.

Keywords:

COMSOL, Vacuum Phototriode, Segmented anode

1. Introduction

Vacuum Phototriodes (VPTs) are single-gain-stage photomultiplier tubes suitable for use or quasi-axial magnetic fields. They have been used in a number of particle physics experiments, such as DELPHI and OPAL for their lead-glass endcap electromagnetic calorimeters [1, 2]. VPTs are currently used to detect scintillation light from the lead tungstate crystals in the endcap electromagnetic calorimeter of the Compact Muon Solenoid (CMS) experiment [3] at CERN's Large Hadron Collider (LHC). VPTs are fast, low-gain devices that can operate in strong magnetic fields at angles up to approximately 40 degrees from the VPT axis of cylindrical symmetry.

A typical VPT consists of three electrodes; photocathode, fine planar anode mesh and dynode in sequence. The dimensions of the VPT currently used in CMS are shown in Fig. 1. The role of the photocathode is to convert light into photoelectrons. The photo-electrons are accelerated to the anode mesh where approximately half pass through to a solid dynode. Secondary electrons generated at the dynode are accelerated and collected at the anode. The induced signal on the anode provides the output of the VPT. An electron microscope has been used to obtain the dimensions of an actual mesh from an RIE FEU-188 VPT (Fig. 2). The mesh has a 10 μm pitch and is approximately 50 % transparent (open area to total area). The VPTs have gains of approximately 10 (number of electrons collected at the anode to the number of photo-electrons emitted) in the 3.8 T magnetic field of CMS. The proximity focusing geometry provides pulses that are fast, with signal rise and fall times of ~ 1 ns [4].

There is an interest in further developing the VPT to have more than one anode within the same diameter of the vacuum envelope for applications that include scintillating or fluorescent fibre based sampling calorimeters [5] typically for applications in an LHC like environment and where the devices would operate at moderate angles to a strong magnetic field, for example in an endcap calorimeter. In this paper, a four-fold segmented anode has been modelled using COMSOL multi-physics software [6] based on a prototype device previously fabricated for us by Hamamatsu. This electrode arrangement of this new VPT differs from the RIE FEU-188 tube as it has a configuration of cathode - dynode - anode (segmented). The COMSOL model was used to compare results with the existing unsegmented anode VPT, and to study optimal designs for the segmented anode.

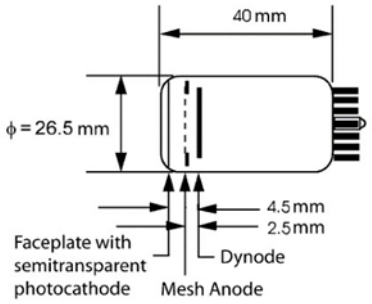

Figure 1 - Outline showing the dimensions of the existing RIE FEU-188 VPT used in the CMS experiment [3].

2. COMSOL Simulation

2.1 FEU-188 VPT

Our simulation of the RIE FEU-188 VPT used the COMSOL Multi-Physics version 5.3 software environment. An image of the anode mesh used in a production device is shown in Fig. 2. This mesh presented a major challenge for the simulation given the fine pitch of 10 μm and the 1.68 μm thickness. The COMSOL simulation required a finite element mesh (FEM) to be created, with many elements that were a factor of one hundred to one thousand times smaller than the separation or diameter of the electrodes. The FEM creates many vertices and boundaries to break down the problem into a simpler form.

This resulted in a number of challenging issues, including boundaries at corners, problems with the minimum element size, and issues with computer memory capacity and computation time. To overcome these issues, the active area of the mesh was reduced to 2×2 mm^2 so that the computational load is reduced. The anode thickness was changed to 2.5 μm in the simulation to avoid meshing errors. The results presented here used a PC with a four-core (plus hyperthreading) Intel i7 processor @3.7 GHz and 48 Gbytes of RAM.

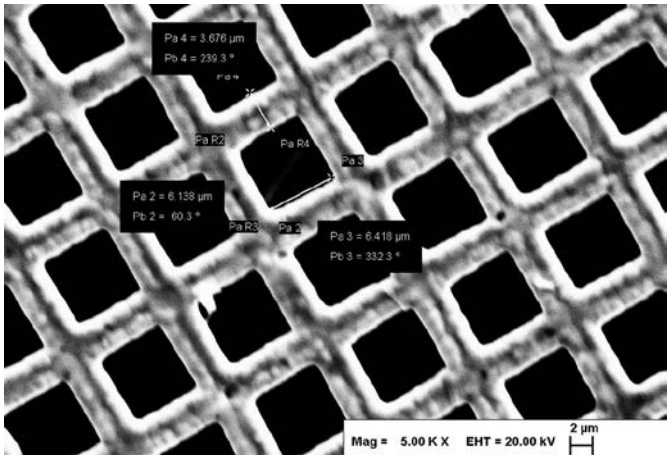

Figure 2 - Image of the anode mesh, removed from an RIE VPT, taken with a scanning electron microscope. The mesh has a 10 µm pitch, thickness of 1.6 µm and is 50% transparent.

The electric potentials within the VPT were as follows; cathode (K) 0 V, anode (A) +1000 V and dynode (D) +800 V. In the actual FEU-188 these potentials result in a gain of approximately ten. In the simulation, electrons were accelerated from the photocathode towards the mesh anode. Those passing through the mesh decelerate to the solid dynode. The secondary electrons produced by the dynode were accelerated back towards the anode. Some of the secondary electrons pass through the anode, decelerate in the anode-cathode region, and are accelerated back towards the anode. A further fraction passes through reaching the dynode, but now with a kinetic energy too low to generate a significant number of further secondary electrons.

The instantaneous current induced on a given electrode, due to the motion of a charge, is given by the Shockley-Ramo theorem [7]:

$$i = -q \cdot \vec{v} \cdot \overrightarrow{F_k} \qquad (1)$$

where $\vec{v} = [v_x v_y v_z]$ is the instantaneous velocity of charge q and $\overrightarrow{F_k}$ is the weighting field that the charge experiences at a distance d to the signal electrode when that electrode is set to unit potential and the other electrodes are set to zero potential.

The current pulse induced on the anode is calculated for a single electron. Examples of simulated, induced anode currents at 0 T are shown in Fig. 3. The dark blue curve shows the induced anode current when an electron is collected at the dynode. The dotted green curve shows the induced anode signal for an electron collected directly at the mesh anode that has not passed through to the dynode. The red curve shows the induced anode current when a secondary electron from the dynode is collected at the anode, producing a peak current of ~ -3 nA. The light blue curve shows the induced anode current when a secondary electron goes through the anode mesh and then accelerates back through the mesh towards the dynode. The results are comparable to previous simulations [4, 8] using a completely different software package SIMION 3D.

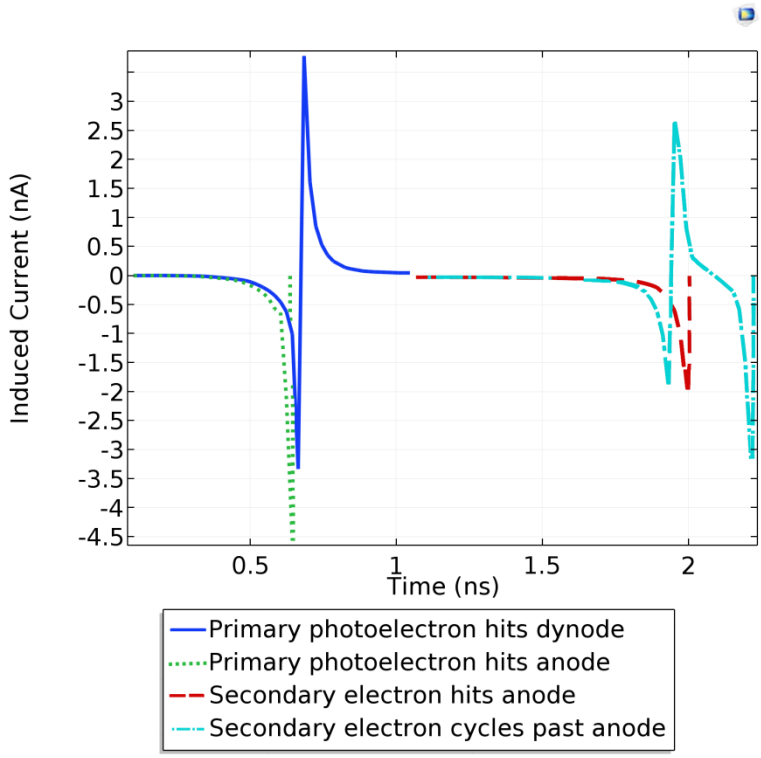

Figure 3 - Simulation of the induced currents in an RIE FEU-188 VPT due to a single electron in 4 different scenarios, with the VPT at 0 T field. The dark blue curve represents the induced current at the anode when the particles go through the anode mesh and collected at the dynode. The dotted green curve represents the induced current on the anode for particles that have not passed through the anode. The red curve represents the induced current at the anode when secondary electrons produced by the dynode are collected at the anode. Finally, the light blue curve represents the case when the secondary emission from the dynode goes back through the anode mesh and returns to the dynode.

The induced currents at 4 T are shown in Fig. 4. When simulating at an angle to the magnetic field only photoelectrons emitted from an offset region of the photocathode that were subsequently transported to the mesh region of the simulated dynode were used. The red curve shows the induced anode current when a secondary electron from the dynode is collected at the anode, producing a peak current of ~ -2.5 nA, which marginally more than the 0 T induced current.

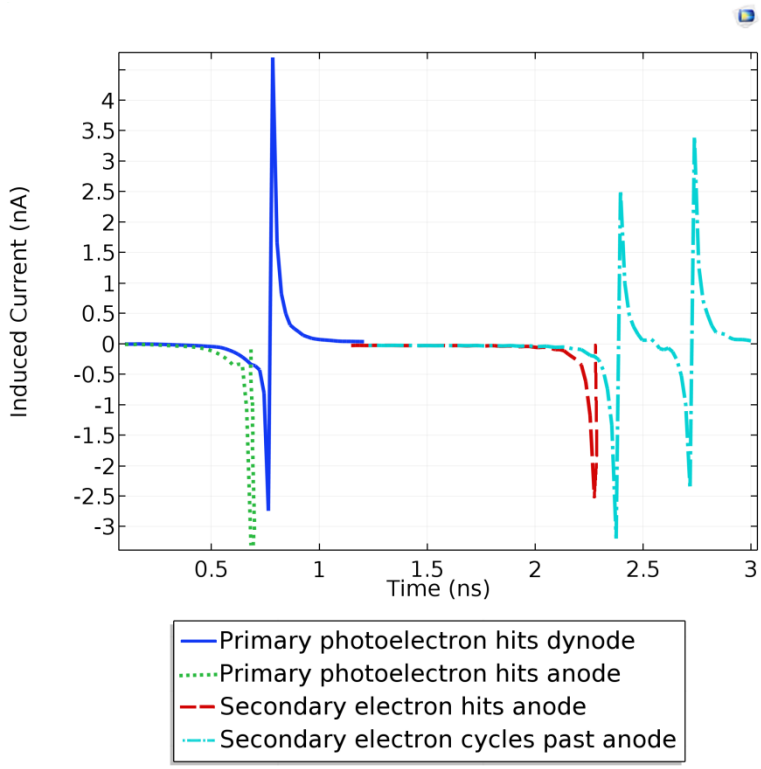

Figure 4 - Simulation of the induced currents in an RIE FEU-188 VPT due to a single electron in 4 different scenarios, with the axis of the VPT at 15° to the 4 T field. The scenarios are identical to those shown in Fig. 3.

2.2. Segmented Anode VPT

Since the VPT is a proximity focused device subdividing the anode or dynode can create several independent channels within the same overall envelope [9]. Such a device could be useful for reading out scintillating or wavelength shifting fibres from a spaghetti calorimetry (SPACAL) type of calorimeter and our work was motivated by this potential application in the endcap region of a detector such as CMS.

A VPT prototype with a segmented anode (type "Triode4", serial number ZG6968) has been produced for us by Hamamatsu. It contains a fine mesh dynode and four independent anodes. It has its circular anode split into four equal quadrants each separated by a 1 mm gap. The device has a transmissive fine mesh dynode between the photocathode and the anode. The construction details of the mesh dynode are not known to us, thus in the model the dynode is approximated as a thin, solid, metal sheet. Fig. 5 shows electron trajectories, and energies in electron volts (represented by the colour scale) at 0 T. The focusing effect seen is due to the influence of an external conducting shield, surrounding the device, which is biased at 0 V. At 4 T this focusing effect is substantially reduced since the electrons follow, and spiral around, the magnetic field lines. The gaps between the anode segments lead to some electrons being transported beyond the anode, as shown in Fig. 6.

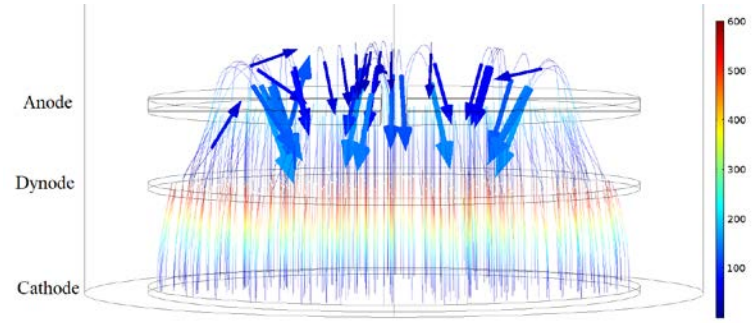

Figure 5 - The trajectories at 0T for photoelectrons travelling from the photocathode via a transmissive dynode towards a segmented solid anode. The particles that pass through the segmented anode gap, are attracted back towards the anode. The colour scale shows the electron energy in electron-volts.

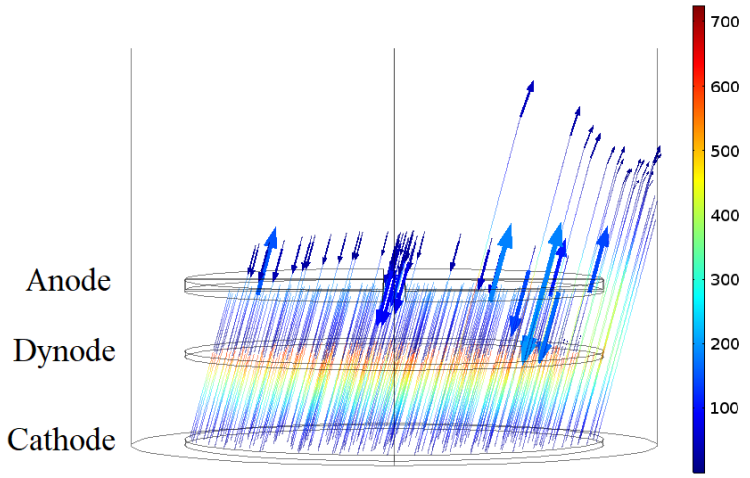

Figure 6 – Particle trajectories at 15° to an axial 4 T field. Approximately 8% of the photoelectrons initially released from the photo-cathode hit the VPT shell. From the secondary emission, approximately 30% of the electrons do not hit the segmented anode. Instead, these electrons either hit the VPT shell or escape through the gaps in between the anode segments. The colour scale shows the electron energy in electron-volts.

The induced current on the anode arising from a single secondary electron from the dynode is shown in Fig. 7. The peak current reaches ~ - 0.6 nA with a rise time just under 1 ns. Fig. 8 shows the induced current from a single electron on the appropriate anode segment (dotted green), and the induced signal (cross-talk) on the adjacent anode segment (blue).

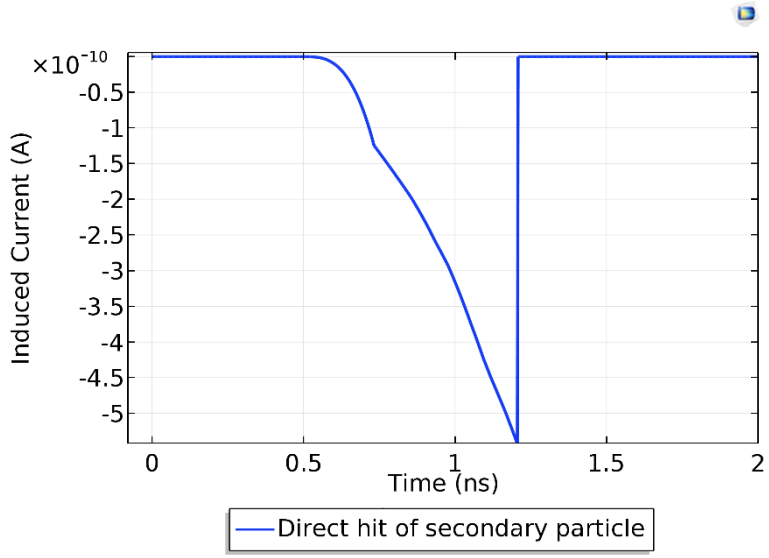

Figure 7 - Induced current at 0 T, on an anode segment from a single secondary electron hitting that segment.

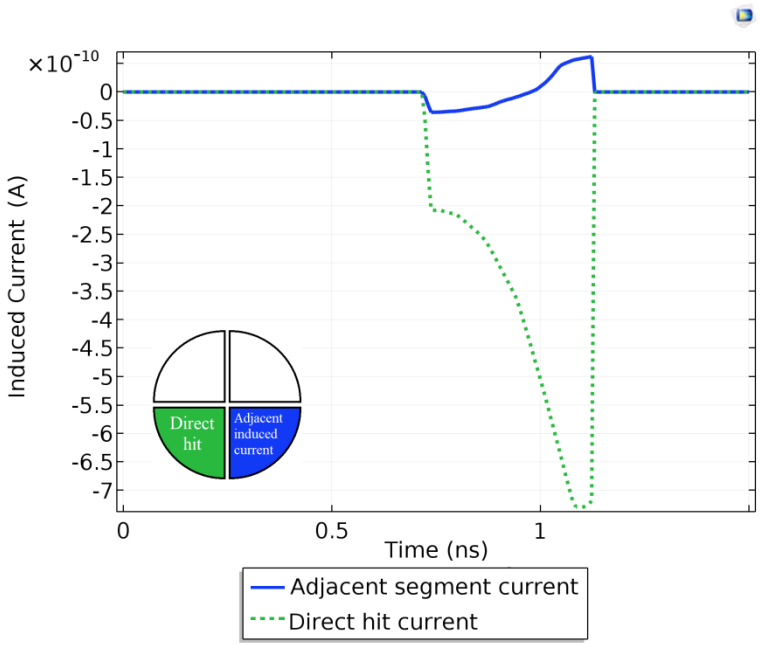

Figure 8 - Induced current at 0 T. From a single electron on the appropriate anode segment (dotted green), and the induced signal (cross-talk) on the adjacent anode segment (blue).

The cross-talk between two adjacent segments is shown in Fig. 9 for a single photo-electron hitting four different locations, labelled A, B, C, D, within one of the segments. The induced current in the adjacent segment (bottom right segment) is calculated using the Shockley-Ramo theorem. Points A, B and C are close to the adjacent segment and induce similar peak crosstalk currents of ~ 0.05 nA, corresponding to ~ 10% of the current in the hit segment. Point D, which is 5 mm from the inter-anode gap, induces a peak crosstalk current of < 0.002 nA (< 0.3%). To minimise crosstalk issues, the fibres from a SPACAL type calorimeter could be arranged such that they only illuminate the central region of each segmented anode avoiding the straight edges of the segment.

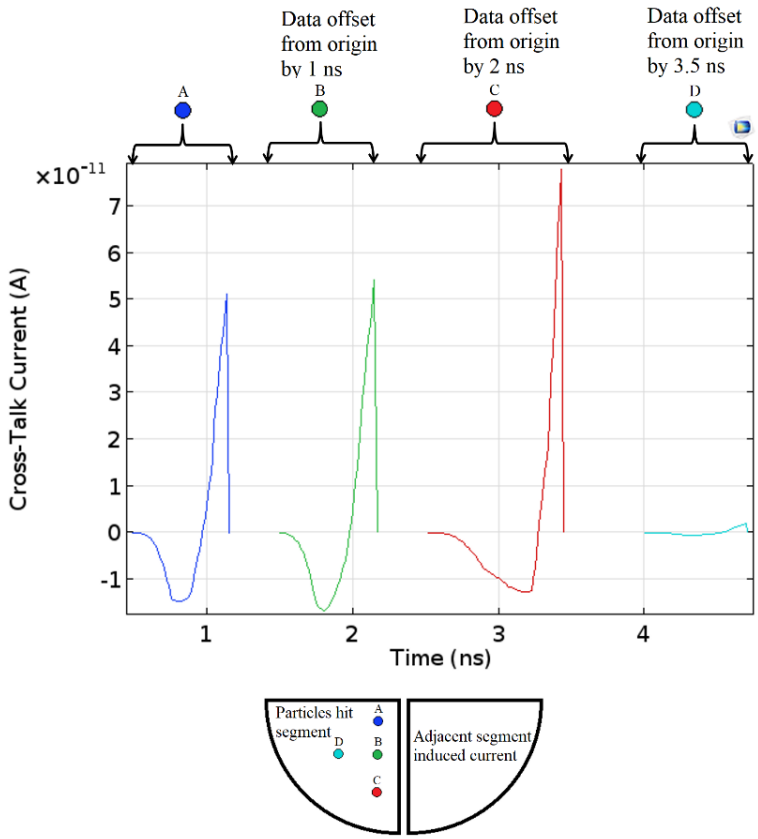

Figure 9 - Simulation of the cross-talk current in a prototype at 0 T. Hamamatsu segmented anode VPT due to a single electron within the lower left segment. The response at points A, B, C and D was studied. The cross-talk current is read from the adjacent segment lower right.

3. Conclusions

A simulation of an RIE FEU-188 VPT was performed with the COMSOL software. The current induced on the mesh anode was calculated using the Shockley-Ramo theorem. The results are compatible with previously published simulations with the SIMION software [4,8]. A prototype VPT manufactured by Hamamatsu, with a fourfold segmented, solid anode, was also simulated. The signal and cross talk on the anodes was determined for illumination on different regions of the photocathode. The simulation predicts that illuminating a restricted region of the photocathode such that photoelectrons will result in secondary electrons, from the dynode, hitting the centre of the anode quadrant is optimum in reducing the cross-talk.

Acknowledgements

One of us (S. Zahid) would like to acknowledge funding for this project via an STFC Doctoral Training award.

References

[1] G. Barichello, M. Mazzucato, M. Pegoraro, G. Zumerle, A low noise amplification chain for the vacuum phototriode readout of the DELPHI leadglass calorimeter, Nuclear Instruments and Methods in Physics Research Section A: Accelerators, Spectrometers, Detectors and Associated Equipment 254 (1) (1987) 111–117.

[2] M. Akrawy, G. T. J. Arnison, Batley, et al., Development studies for the OPAL end cap electromagnetic calorimeter using vacuum photo triode instrumented leadglass, Nuclear Instruments and Methods in Physics Research Section A: Accelerators, Spectrometers, Detectors and Associated Equipment 290 (1) (1990) 76–94.

[3] CMS Collaboration, "Performance and operation of the CMS electromagnetic calorimeter," Journal of Instrumentation, vol. 5, no. 03, p. T03010, (2010).

[4] D. E. Leslie, I. Yaselli, P. R. Hobson, Timing performance of a vacuum phototriode, Astroparticle, Particle and Space Physics, Detectors and Medical Physics Applications (2007) 90.

[5] N. Akchurin, F. Bedeschi, A. Cardini, et al., The electromagnetic performance of the RD52 fiber calorimeter, Nuclear Instruments and Methods in Physics Research Section A: Accelerators, Spectrometers, Detectors and Associated Equipment 735 (2014) 130–144. doi: http://dx.doi.org/10.1016/j.nima.2013.09.033.

[6] Comsol multiphysics ^{R} v. 5.3, www.comsol.com, COMSOL AB, Stockholm, Sweden.

[7] W. Shockley, Currents to conductors induced by a moving point charge, Journal of applied physics 9 (10) (1938) 635–636.

[8] I. Yaselli, Studying the Time Response of a Vacuum Phototriode and Measurement of Gamma Radiation Damage to High Voltage Capacitors and Resistors, Ph.D. thesis, Brunel U. (2008).
URL http://bura.brunel.ac.uk/handle/2438/3018

[9] H. Kume, S. Suzuki, J. Takeuchi, K. Oba, Newly developed photomultiplier tubes with position sensitivity capability, IEEE Transactions on Nuclear Science 32 (1) (1985) 448–452.